International Journal of Mechanical Engineering and Robotics Research

ISSN 2278 – 0149 www.ijmerr.com
Vol. 1, No. 3, October 2012

Research Paper

NUMERICAL INVESTIGATION OF AERODYNAMIC CHARACTERISTICS OF NACA 23018 AIRFOIL WITH A GURNEY FLAP

MasoudJahanmorad Nouri[1]*, Habibollah Sayehvand[1] and Abolghasem Mekanik[1]

Corresponding Author: **MasoudJahanmorad Nouri, ✉ masoud_jnouri@yahoo.com*

A two-dimensional numerical investigation was performed to determine the effect of a Gurney flap on a NACA 23018 airfoil. An incompressible Navier-Stokes solver with Spalart-Allmaras turbulence model is used to predict the flow field around the airfoil. Gurney flap sizes of 0.5%, 1.0%, 1.5%, 2.0%, and 3.0% of the airfoil chord were studied.Computed results have been compared with available experimental data. Addition of Gurney flap increases the lift coefficient significantly with very little drag penalty if proper Gurney flap height is selected. Results showed that Gurney flaps produced a negative shift in the zero-lift angle of attack. The numerical solutions show the details of the flow structure at the trailing edge and provide a possible explanation for the increased aerodynamic performance.

Keywords: Gurney flap, Lift enhancement, NACA23018 airfoil, Computational fluid dynamics

INTRODUCTION

High lift systems play a major role in performance and economic success of commercial, transport and military aircraft. An efficient high lift system offers many advantages like lower take off and landing speed, greater payload capacity for given wing, longer range for given gross weight and higher manoeuvrability. High lift systems are desired to maintain low drag at take off so as to attain cruise speed faster and high drag at approach. High lift systems are often quite complex consisting of many elements and multi bar linkages. Therefore there is need to have simpler high lift systems which are cheaper in terms of manufacturing and maintenance cost. One such candidate is Gurney flap.

The Gurney flap is a simple device, consisting of a short strip, on the order of 1-5% of the airfoil chord in height, fitted perpendicular to the pressure surface or the chord-line along the trailing edge of a wing (Figure 1). The most common application of this device is in racing-car spoilers, where it is used to increase the down-force.

[1] Mechanical Engineering Department, School of Engineering, Bu-Ali Sina University, Hamedan.

Figure 1: NACA 23018 Profile Fitted with a Gurney Flap

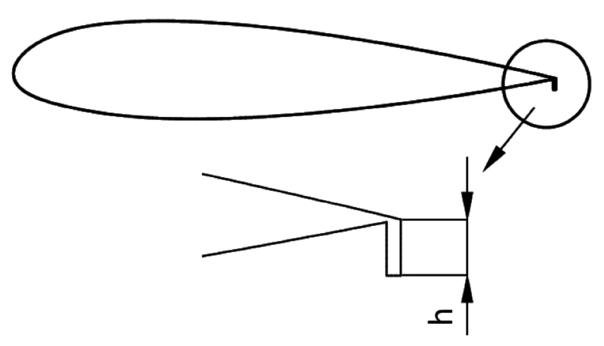

Note: h – Gurney Flap Height.

Liebeck (1978) conducted wind tunnel tests on the effect of a 1.25% C height Gurney flap on a Newman airfoil, which resulted in an increase in lift and a slight reduction in drag. Larger lift increments were observed for greater flap heights, but the drag increased noticeably beyond heights of approximately 2% C. Liebeck (1978) also hypothesized on the changes in the trailing edge flow field caused by the Gurney flap (Figure 2), and this assumption was based on the trailing edge flow field for a clean airfoil reported by Kuchemann (1967). When a tufted probe was used by Liebeck (1978), a considerable turning of the flow over the back side of the flap was observed.

Figure 2: Hypothesized Trailing Edge Flow Conditions of an Airfoil with a Gurney Flap

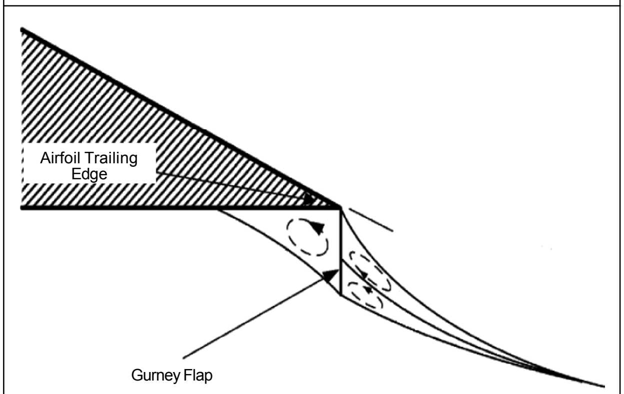

Source: Liebeck (1978)

Gurney flaps dramatically increase lift without degradation of the airfoil performance when the height of Gurney flap is less than the boundary layer thickness. Until now, the flow control effect of Gurney flap has been investigated by several researchers (Storms and Jang, 1994; and Myose *et al.*, 1998). The results showed that compared to a clean airfoil, Gurney flap reduces the pressure on the suction side and increases the pressure on the pressure side. These pressure variations are induced by the enhancement of circulation related to the extra downward turning of the flow generated behind the Gurney flap. As a result of the pressure variations, additional pressure difference between the upper and lower surfaces occurs, and this causes the increment of the maximum lift, the decrement of the zero-lift angle of attack, and the increment of the nose-down pitching moment, similar to the effect of increasing the camber of the airfoil (Myose *et al.*, 1998). The amount of lift increment is proportional to the height of the Gurney flap. But when the height exceeds the boundary layer thickness, the drag also increases. Therefore the flap height should be determined in a way that the maximum lift-to-drag ratio can be achieved.

In more recent studies, articulated Gurney flap-like devices have been used to tailor the spanwise loading of wings (Bieniawski and Kroo, 2003) and rotor blades (Thiel *et al.*, 2006).

The objective of the present study is to provide quantitative and qualitative computational data on the performance of the Gurney flap. Computations of a baseline

NACA 23018 airfoil are compared with experimental results obtained in the Langley two-dimensional low-turbulence pressure tunnel by Abbott *et al.* (1945). Subsequent computations were performed to determine the effect of various sizes of Gurney flaps on the lift and the drag of the same airfoil.

MATERIALS AND METHODS

Numeric Simulation

Computational Fluid Dynamics (CFD) is generally understood to be any numerical method used to solve a set of equations to model the flow-field of study. For this case, Fluent was used to solve the Incompressible Navier-Stokes equations (INS).

The continuity equation can be expressed as:

$$\nabla \cdot u = 0 \qquad \text{...(1)}$$

The next set of equations establishes a conservation of momentum in each spatial dimension. In the current 2D study, only equations for the x and y direction were solved. The equations can be expressed as:

$$\frac{\partial u}{\partial t} + u \cdot \nabla u + \frac{1}{\rho}\nabla P = \vartheta \nabla^2 u + f \qquad \text{...(2)}$$

The equations are solved by the commercial code Fluent. The nonlinear system of equation implies the segregated solver, thus is solved sequentially. Standard and Second Order Upwind discretization schemes are used for the continuity and the momentum equations respectively.

As the code solves the incompressible flow equations, no equation of state exist for the pressure, and a SIMPLE algorithm is used to enforce pressure-velocity coupling.

Geometry Modeling and Grid Generation

The geometry used for the Gurney flap study is a NACA 23018 airfoil. Computations were performed for Gurney flap sizes ranging from 0.5% to 3% chord length, with the flaps located on the windward side of the airfoil at the trailing edge. For simplicity, the wind tunnel walls used for the experiment were not modeled.

For NACA23018 airfoil, computations were performed using a C-grid as shown in Figure 3. The top and bottom farfield boundaries are twelve chord lengths from the airfoil; the upstream and downstream boundaries are eleven and twenty chord lengths away, respectively. The grid was constructed using the Gambit software. Figure 4 shows a closer view of the grid in the vicinity of the airfoil. Grid clustering is evident near the surface of the airfoil, as well as near the trailing edge, to obtain reasonable resolution of the boundary layer and the region around the Gurney flap. Figure 5 shows a grid with a 2% Gurney flap at the airfoil trailing edge.

Figure 3: C-Grid Used for NACA23018 Airfoil

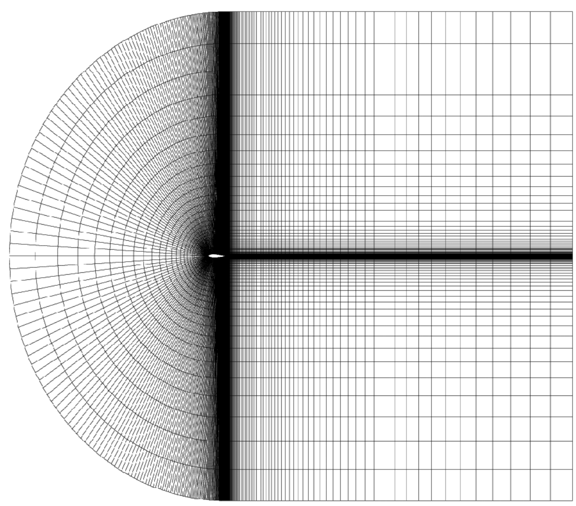

Figure 4: Close Up of Grid in the Vicinity of NACA 23018 Airfoil

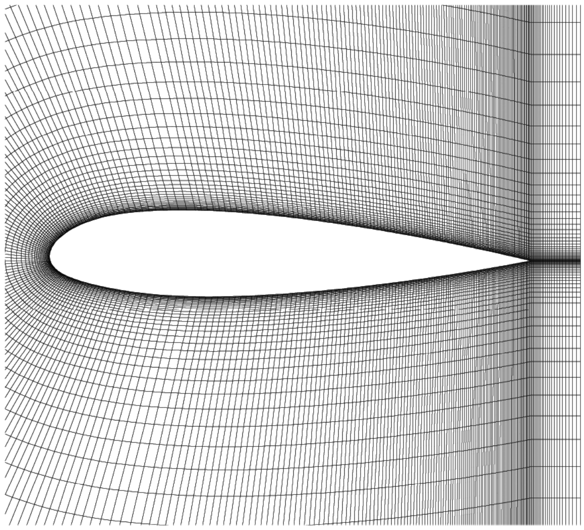

Figure 5: Details of Grid in the Vicinity of the Trailing Edge NACA 23018 Airfoil with a 2% C Gurney Flap

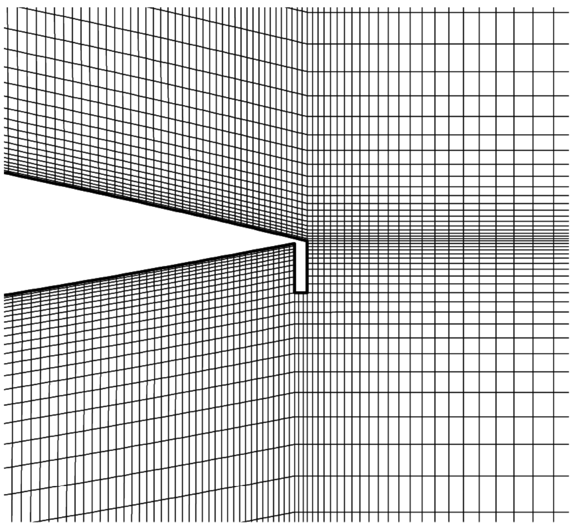

RESULTS AND DISCUSSION

Computations were performed for a NACA 23018 airfoil at conditions which match the experimental data of Abbott *et al.* (1945). The Reynolds number for the computational cases matches the experimental Reynolds number, based on wing chord, of $Re_c = 3.1 \times 10^6$. The wind tunnel test was performed in the Langley two-dimensional low-turbulence pressure tunnel.

Experimental results are compared with computational resultsfor the baseline airfoil in Figure 6 (no Gurney flap simulation). The results agree well with the measured data up to $\alpha \approx 14°$. While this is the point of maximum lift for the NACA 23018 airfoil (C_{lmax} = 1.38), the Fluent with the Spalart-Allmaras turbulence model predicts that the maximum lift coefficient occurs at α = 14° (C_{lmax} = 1.37). Since the Gurney flapswill be simulated at angles of attack below stall, this comparison shows that the Navier-Stokes solutions are simulating the pre-stall flowfield quite well. Figure6 also shows comparisons between experimental and computational drag coefficients. There is general agreement with the experimental data.

Figure 6: Comparison of Computed Lift and Drag Coefficients with Experimental Data; NACA 23018 Airfoil (Base Line), $Re_c = 3.1 \times 10^6$, α = 0°, 2°, 4°, ..., 18°

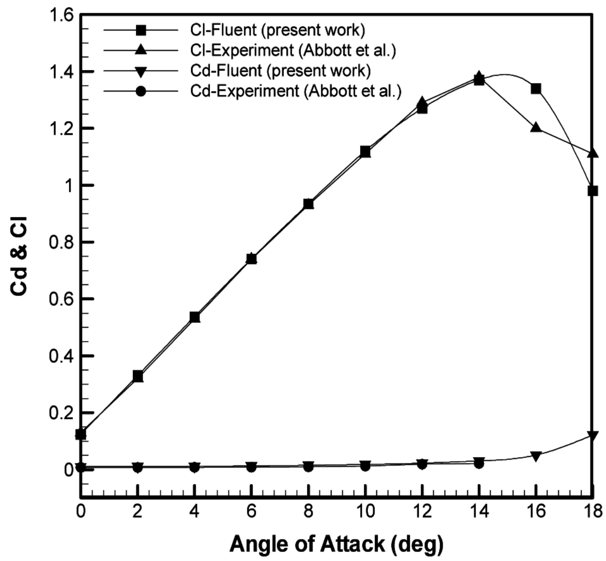

Figure 7 shows the lift coefficient results for the NACA 23018 airfoil with different size

Figure 7: Effect of Gurney Flap Size on Lift Coefficient; NACA 23018 Airfoil (Base Line Case and with Gurney Flap Size of *h* = 0.5% C, 1% C, 1.5% C, 2% C and 3% C), $Re_c = 3.1 \times 10^6$, $\alpha = 0°, 2°, 4°, ..., 16°$

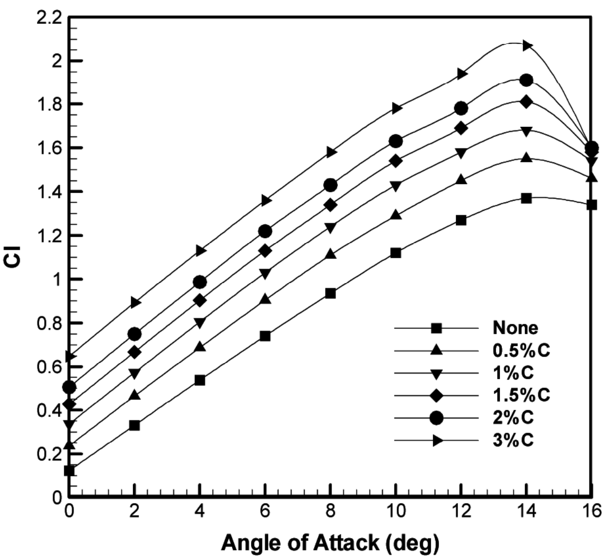

Figure 8: Effect of Gurney Flap Size on Drag Coefficient; NACA 23018 Airfoil (Base Line Case and with Gurney Flap Size of *h* = 0.5% C, 1% C, 1.5% C, 2% C and 3% C), $Re_c = 3.1 \times 10^6$, $\alpha = 0°, 2°, 4°, ..., 16°$

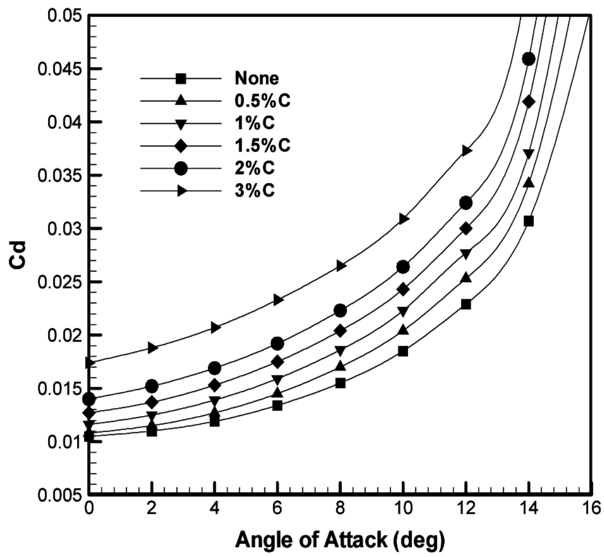

Gurney flaps. In general, the lift coefficient increases as the Gurney flap size increases for a given angle of attack. As an example, a 1% chord Gurney flap shifts the lift curve by more than 3°, but the relationship between the Gurney flap size and lift-curve shift does not appear to be linear. Specifically, the increase in lift coefficient due to changing the Gurney flap size from 0% to 0.5% chord is greater than the change found by changing the flap from 1.5% to 2% chord. The figure also shows that the zero lift angle of attack appears to become increasingly more negative as a larger Gurney flap is utilized. These results suggest that the effect of the Gurney flap is to increase the effective camber of the airfoil.

Shown in Figure 8 is the drag polar for the same configurations. The significant increase in lift coefficient for the 3% height Gurney flap comes at the price of substantially increased drag as shown in Figure 8.

Figure 9 presents the polar of lift-to-drag ratio versus lift coefficient. At low-to-moderate lift coefficients (C_l < 1.2), there is a drag

Figure 9: Lift-to-Drag Ratio vs. Lift Coefficient NACA 23018 Airfoil (Base Line Case and with Gurney Flap Size of h = 0.5% C, 1% C, 1.5% C, 2% C and 3% C), $Re_c = 3.1 \times 10^6$, $\alpha = 0°, 2°, 4°, ..., 16°$

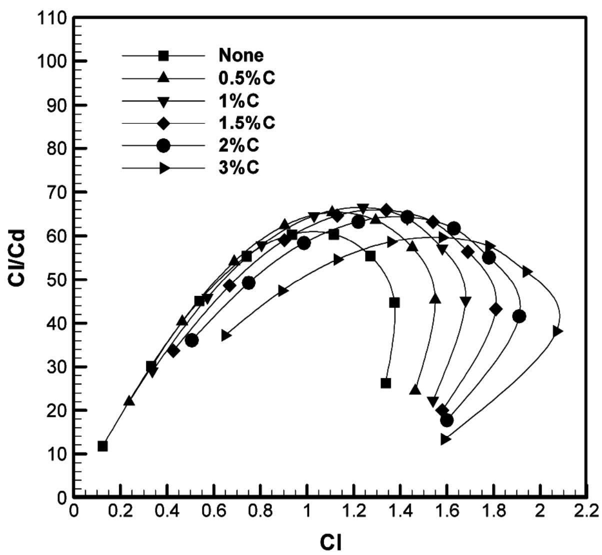

penalty associated with the Gurney flap which increased with flap height. At higher lift coefficients ($C_l \geq 1.2$), however, the lift-to-drag ratio is significantly increased. When the lift coefficient is about 1.37, the increment of lift-to-drag ratio, approximate 43%, was obtained by the 2% C Gurney flap. As a result, the effect on the maximum lift-to-drag ratio is small, but the lift coefficient for a given lift-to-drag ratio is significantly increased.

Pressure distributions for the clean airfoil and the 2% C height Gurney flap at three different angles of attack are shown in Figure 10. Using the Gurney flap, Figure 10 shows

Figure 10: Comparison of Pressure Coefficient NACA 23018 Airfoil (Base Line Case and with Gurney Flap Size of h = 2% C), $Re_c = 3.1 \times 10^6$

(a) α = 0°

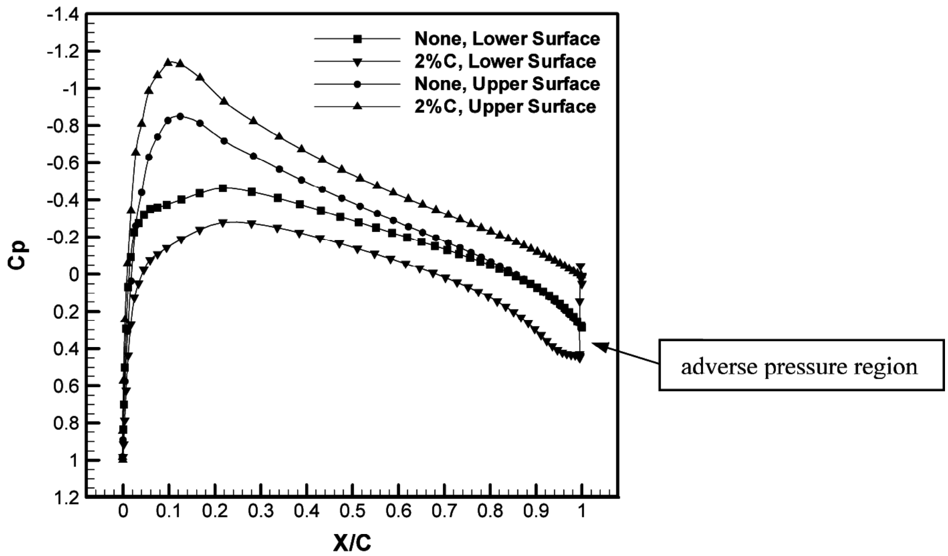

(b) α = 6°

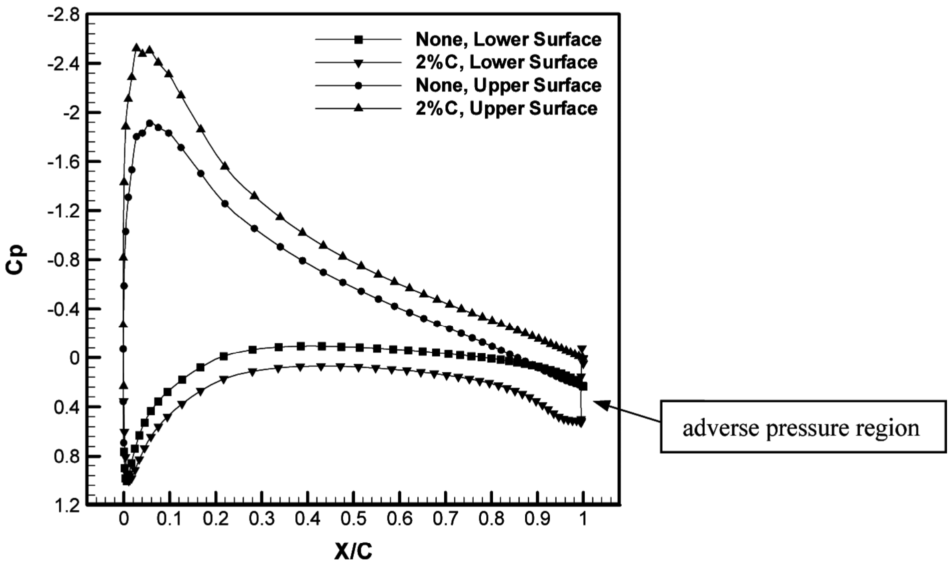

Figure 10 (Cont.)

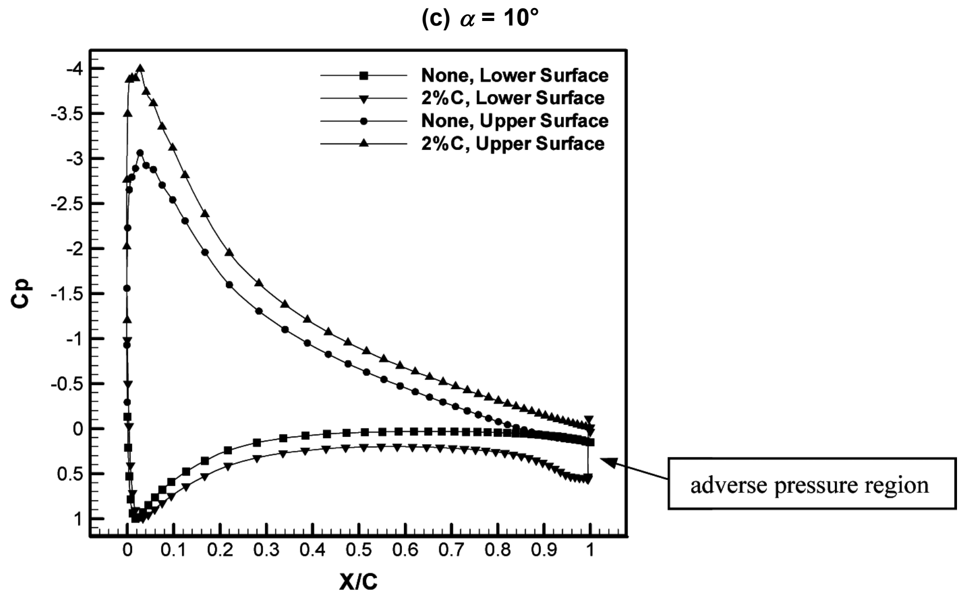

that the increased suction is evident everywhere on the upper surface while the lower surface experiences increased pressure. This results in the substantially increased lift coefficient with the Gurney flap which was discussed earlier. Note the adverse pressure surface due to the presence of the Gurney flap. Such an adverse pressure region is to be expected in front of the flap, and was found in all previous studies with pressure distribution measurements (Katz and Dykstra, 1989; Giguère *et al.*, 1995; and Myose *et al.*, 1996). Liebeck (1978) has theorized that a recirculating vortex may be associated with this adverse pressure region just upstream of the flap on the lower surface, as shown in Figure 2.

The computed flowfieldin the vicinity of the trailing edge is shown in Figure11 for α = 6°

Figure 11: Computed Stream Lines Around Trailing Edge of the NACA 23018 Airfoil; $Re_c = 3.1 \times 10^6$, $\alpha = 6°$

(a) Airfoil with No Gurney Flap

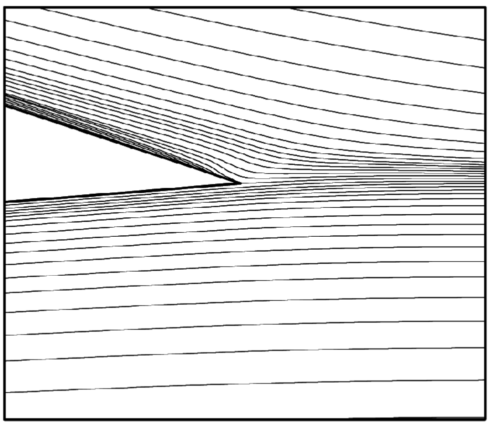

(b) Airfoil with 2% Chord Gurney Flap

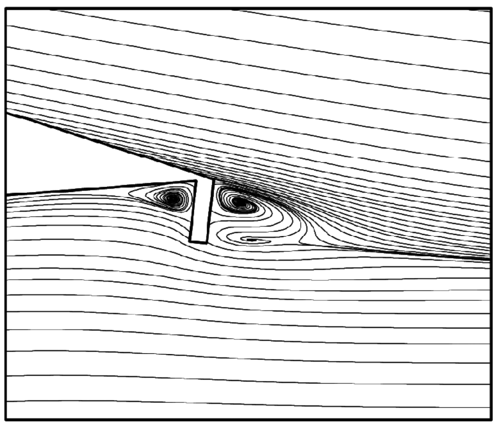

with and without a 2% chord Gurney flap. A recirculation region can be seen in front of the flap and a strong clockwise vortex is apparent on the upper backside of the flap. It is observed from the flow fields comparison (a) and (b) that Gurney flap causes flow to turn downward beyond the flap, which indicates that increased lift is being generated by the Gurney flap. This is in agreement with Liebeck's (1978) wind tunnel test, where tufted probe indicated significant turning of the flow downstream of the flap. The adverse pressure gradient observed upstream of the flap on the lower surface may be attributed to the formation of recirculating cove vortex.

CONCLUSION

A computational study of the flowfieldpast NACA 23018 airfoil with Gurney flap has been conductedin detail using the commercial code Fluentwith the one-equation turbulence model of Spalart-Allmaras. Computational results are found to agree reasonably well with available experimental data. Results showed that Gurney flaps produced a positive increment in lift coefficient, a negative shift in the zero-lift angle of attack and a drag increment compared to those obtained for clean airfoil, however these increments are nonlinear with respect to flap height. There is no significant increase in drag if Gurney flap height is kept within boundary layer, however beyond this limit drag increment is significant. Airfoil pressure distribution results show that the Gurney flap increases the upper surface suction and the lower surface high pressure, this is the reason why the lift can be enhanced. The flowfield in the vicinity of the trailing edge shows that the addition of the Gurney flap results in a downward turning of the flow behind the airfoil, so that the Gurney flap increases the effective camber of the airfoil.

REFERENCES

1. Abbott Ira H, Von Doenhoff Albert E and Stivers Louis S Jr. (1945), "Summary of Airfoil Data", NACA Rep. No. 824.
2. Bieniawski S and Kroo I (January 2003), "Development and Testing of an Experimental Aeroelastic Model with Micro-Trailing Edge Effectors", American Institute of Aeronautics and Astronautics (AIAA) 2003-220.
3. Giguère P, Lemay J and Dumas G (1995), "Gurney Flap Effects Scaling for Low-Speed Airfoils", American Institute of Aeronautics and Astronautics (AIAA) Paper 95-1881.
4. Katz J and Dykstra L (1989), "Study of an Open-Wheel Racing Car's Rear-Wing Aerodynamics", Paper Presented at the SAE International Congress and Exposition, February 27-March 3, SAE Paper 890600, Detroit, MI.
5. Kuchemann D (1967), "Inviscid Shear Flow Near the Trailing Edge of an Airfoil", *Z. Flugwiss*, Vol. 15, pp. 292-294.
6. Liebeck R H (1978), "Design of Subsonic Airfoils for High Lift", *J. Aircraft*, Vol. 15, pp. 547-561.
7. Myose R, Heron I and Papadakis M (1996), "The Post-Stall Effect of Gurney Flaps on a NACA-0011 Airfoil", Aerospace Atlantic Conference, May 22-23, SAE Paper 961316, Dayton, Ohio.
8. Myose R, Papadakis M and Heron I (1998), "Gurney Flap Experiments on

Airfoils, Wings and Reflection Plane Model", *J. Aircraft*, Vol. 35, No. 2, pp. 206-211.

9. Storms B L and Jang C S (1994), "Lift Enhancement of an Airfoil Using a Gurney Flap and Vortex Generators", *J. Aircraft*, Vol. 31, No. 3, pp. 542-547.

10. Thiel M R, Lesieutre G A, Maughmer M D and Koopmann G H (May 2006), "Actuation of an Active Gurney Flap for Rotorcraft Application", American Institute of Aeronautics and Astronautics (AIAA) 2006-2181.

APPENDIX

Nomenclature	
C	Chord length
C_d	Drag coefficient
C_l	Lift coefficient
C_p	Pressure coefficient
f	Body force
P	Pressure
Re	Reynolds number
t	Time
u	Velocity
α	Angle of attack
ϑ	Kinematic viscosity
ρ	Density
∇	Divergence